interventions. Computed tomography (CT), which shows high temporal and spatial resolution, has been used to detect selective muscle involvement, such as atrophy or fatty tissue replacement, in patients suffering from DMD,[16,17] but it requires ionizing radiation and has limited sensitivity for soft tissues.[18] Magnetic resonance imaging (MRI) produces high-resolution images with good contrast among soft tissues,[19] and therefore it has been used to evaluate skeletal muscle involvement in DMD[20] and in *mdx* mice.[21] In the early stages of dystrophy, the T1 relaxation time is prolonged due to muscle degeneration and regeneration together with an increase in muscle water concentration, and it is decreased owing to fat infiltration in the advanced stage.[22] As the main magnetic field increases, however, the capacity to differentiate tissues on the basis of T1 relaxation time may decrease.[23] On the other hand, the T2 relaxation time is prolonged in necrotic as well as fatty and connective tissue[19]; therefore, it can hardly distinguish necrosis from fat replacement or fibrosis during the dystrophic process. To selectively detect necrotic changes, MR contrast agents, such as gadolinium diethylenetriamine pentaacetic acid (Gd-DTPA), have been used extensively,[24–26] but these agents may also enhance blood vessels and the interstitium,[27] and may cause severe adverse effects, such as anaphylaxis,[28,29] which are critical for DMD patients. Thus, a safer imaging protocol is needed to distinguish necrotic lesions from fatty degeneration or fibrosis in the dystrophic skeletal muscle of DMD and $CXMD_J$.

To discriminate necrosis from fatty infiltration, one of the fat suppression sequences may be useful. As a fat suppression sequence, short-tau inversion recovery (STIR) MR imaging was used to detect muscle edema in DMD.[6] However, STIR suppresses the signal from any tissue or fluid that has a short T1 relaxation time, and therefore it does not selectively suppress the fat signal.[30,31] In contrast, chemical shift selective (CHESS) imaging, another fat suppression sequence, is a technique that selectively saturates fat magnetization by applying a 90° pulse matching with the fat resonance frequency and therefore leads to a highly selective suppression of fat signals. Moreover, the signal-to-noise ratio (SNR) of CHESS is better than that of STIR at a higher magnetic field. The sequence of CHESS combined with T2-weighted imaging (CHESS-T2WI) has been used to diagnose disorders such as lipomatous tumor or temporomandibular arthrosis.[32–34] The method, however, has not been applied to evaluation of the dystrophic changes seen in DMD or the animal models to date.

We, therefore, examined dystrophic dog muscle by CHESS-T2WI to determine whether this sequence is more useful for finding necrosis and inflammatory change than the conventional sequences of T2WI or contrast imaging.

METHODS

Animals. We used three 3-month-old normal male dogs (II-2308MN, II/III-3911MN, and II-4202MN), three littermate $CXMD_J$ male dogs (II-2302MA, II/III-3903MA, and II-4204MA), one 7-year-old normal male dog (00-174MN), and two 7-year-old $CXMD_J$ male dogs (II-C04MA and II-C12MA). II-2308MN, II-4202MN, II-2302MA, and II-4204MA were produced by mating a second-generation (G2) carrier female[13] and G2 affected male. II/III-3911MN and II/III-3903MA were the offspring of a G2 carrier female and a third-generation (G3) affected male. We obtained II-C04MA and II-C12MA by mating first-generation (G1) carrier female dogs and pure-bred normal male Beagles. 00-174MN was a pure-bred normal Beagle. All dogs were part of the breeding colony at the General Animal Research Facility, National Institute of Neuroscience, National Center of Neurology and Psychiatry (Tokyo, Japan), or the Chugai Research Institute for Medical Science, Inc. (Nagano, Japan). Ages, body weights, and serum creatine kinase values at the time of MRI of each dog are shown in Table 1. This study was carried out according to the guidelines provided by the Ethics Committee for the Treatment of Middle-sized Laboratory Animals of the National Center of Neurology and Psychiatry (Approval Nos. 18-02, 19-02, and 20-02).

MR Scanning and Image Analysis. General anesthesia was induced by an intravenous injection of thiopental sodium (20 mg/kg) before MRI scanning and was maintained by inhalation of isoflurane (2.0–3.0%). We examined lower leg muscles of these dogs by superconducting 3.0-Tesla MRI (Magnetom Trio; Siemens Medical Solutions, Erlangen, Germany) with a human extremity coil 18 cm in diameter. The MRI pulse sequences used were T1-weighted imaging (T1WI), T2WI, chemical shift selective T1-weighted imaging (CHESS-T1WI), CHESS-T2WI, gadolinium-enhanced T1-weighted imaging (Gd-T1WI), chemical shift selective gadolinium-enhanced T1-weighted imaging (CHESS-

Table 1. Clinical profiles of normal and dystrophic male dogs used in this study.

	Age (mo)	BW (kg)	Serum CK (IU/L)
Normal dogs			
II-2308MN	3	6.8	197
II/III-3911MN	3	7.7	318
II-4202MN	3	5.8	274
00-174MN	87	13.7	83
CXMDJ dogs			
II-2302MA	3	7.2	30,200
II/III-3903MA	3	6.6	22,300
II-4204MA	3	6.0	28,800
II-C04MA	85	11.5	6500
II-C12MA	94	11.6	1602

Body weight (BW) and serum creatine kinase (CK) values were measured on the day of MRI examination.

Gd-T1WI), and multi-echo T2WI for calculation of T2 relaxation time. In contrast-enhanced images, we injected 0.2 ml/kg of the gadolinium-based MR contrast agent Gd-DTPA (Magnevist; Bayer Schering Pharma, Berlin, Germany) for each sequence. In 3-month-old dogs, we scanned the images for 26 minutes, about 5 minutes after the intravenous injection. On the other hand, we took the images for 13 minutes in 7-year-old dogs at 25 minutes after the injection in order to minimize the risk of anesthesia on the cardiac involvement seen in advanced $CXMD_J$.[15] CHESS was employed to assess necrotic and inflammatory changes more precisely. The acquisition parameters for T1WI, CHESS-T1WI, Gd-T1WI, and CHESS-Gd-T1WI were based on spin echo: repetition time (TR)/echo time (TE) = 500/7.4 ms; slice thickness = 4 mm; field of view = 18 × 18 cm; matrix = 256 × 256; and NEX = 3. The parameters for T2WI and CHESS-T2WI were chosen based on fast spin echo: TR/TE = 4000/85 ms; slice thickness = 4 mm; field of view = 18 × 18 cm; matrix = 256 × 256; turbo-factor = 9; and NEX = 3. The parameters for multi-echo T2WI were selected based on spin echo: TR = 2000; TE = 11.8–118.0 (10 echoes); slice thickness = 4 mm; field of view = 28 × 28 cm; matrix = 256 × 256; and NEX = 2. We were able to clearly distinguish each lower leg muscle by each sequence. Representative cross-sectional images and anatomical locations of lower leg muscles by CHESS-T1WI in a 7-year-old normal dog are shown in Figure 1.

For quantitative analysis of the images, the manufacturer's software (Syngo MR2004A; Siemens Medical Solutions, Erlangen, Germany) was used. Flow artifacts were slight, but regions of interest (ROIs) were selected to avoid flow artifacts and large vessels as follows: three circular ROIs were picked in both right tibialis cranialis (Rt. TC) and extensor digitorum longus (Rt. EDL) muscles of the 3-month-old dogs. ROIs were also selected in the Rt. TC of the 7-year-old dogs and a normal dog. Then, T2 relaxation time or signal intensities (SIs) of CHESS-T1WI, CHESS-Gd-T1WI, and CHESS-T2WI were measured in these ROIs. Signal-to-noise ratios (SNRs) of each ROI were calculated by the equation: $SNR = SI/SD_{air}$, where SD_{air} was the standard deviation (SD) of background noise.[35] The contrast enhancement (CE) ratio was calculated using the SNR of CHESS-T1WI ($SNR_{precontrast}$) and SNR of CHESS-Gd-T1WI ($SNR_{postcontrast}$) by the following equation: $CE = SNR_{postcontrast}/SNR_{precontrast}$. We used the means of the quantitative values at three points of ROIs for statistical analysis.

Statistical Analysis. The T2 relaxation time, CE ratio, and SNR of CHESS-T2WI were evaluated using a one-way analysis of variance (ANOVA) to determine differences among the groups. When a significant difference was found with one-way ANOVA, intergroup comparisons were undertaken using Fisher's protected least significant difference test. All values are expressed as mean ± SE, and statistical significance was recognized at $P < 0.05$.

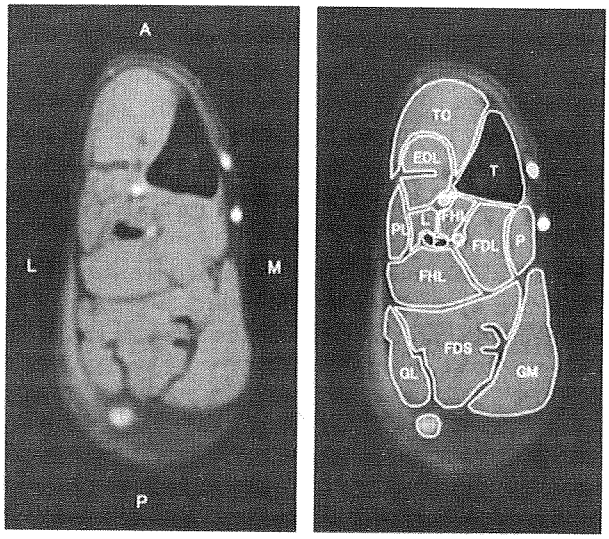

FIGURE 1. Cross-sectional images and anatomical orientation of right lower leg muscles of a 7-year-old normal dog in CHESS-T1WI. A 7-year-old normal dog (00-174MN) was used for this study. T, tibia; F, fibula; TC, tibialis cranialis; EDL, extensor digitorum longus; FHL, flexor hallucis longus; FDL, flexor digitorum longus; FDS, flexor digitorum superficialis; GM, gastrocnemius medialis; GL, gastrocnemius lateralis. A, anterior; P, posterior; L, lateral side; M, medial side.

Histopathology. We performed muscle biopsies of the right TC and right EDL on a 3-month-old normal dog (II-2308MN) and a $CXMD_J$ dog (II-2302MA), and right TC on a 7-year-old normal dog (00-174MN) and a $CXMD_J$ dog (II-C04MA) after MRI scanning. The muscle samples were snap-frozen in liquid nitrogen cooled by isopentane. Hematoxylin and eosin (H&E) staining was performed on serial 10-μm transverse cryostat sections. Anti-IgG immunofluorescence staining was performed on 6-μm serial cryostat sections incubated with fluorescein isothiocyanate (FITC)-conjugated polyclonal sheep anti-canine IgG (1:200; AbD Serotec, Oxford, UK) overnight. To examine fatty infiltration in the muscle, 6-μm serial frozen sections from normal and $CXMD_J$ dogs at 7 years of age were stained with oil red O.

RESULTS

MRI Findings of Lower Leg Muscles in 3-Month-Old Normal Dogs. First, we acquired muscle images of three 3-month-old normal dogs by T1WI, T2WI, CHESS-T1WI, CHESS-T2WI, Gd-T1WI, and CHESS-Gd-T1WI. Representative cross-sectional images of II-2308MN are shown in Figure 2A. In normal dogs, the lower leg muscles showed a homogeneous signal intensity in these sequences, but the muscles that contain mainly slow-twitch fibers, such as the gastrocnemius (GC) and flexor digitorum superficialis (FDS) (Fig. 2A, e and i), showed slight hyperintensity on T2WI and CHESS-T2WI when compared with muscles that contain mainly fast-twitch fibers such as TC and EDL (Fig. 2A, e and i). These findings were consistent with the previous T2 relaxation time study of rabbit muscles.[36] Gd-T1WI (data not shown) or CHESS-Gd-T1WI (Fig. 2A, g) showed homogeneous and slight enhancement when compared with T1WI (Fig. 2A, a) or CHESS-T1WI (Fig. 2A, c), respectively, in all normal dogs.

MRI Findings of Lower Leg Muscles in 3-Month-Old Dystrophic Dogs. Next, we tried to detect muscle involvement in three 3-month-old $CXMD_J$ dogs. Clinically, the dogs showed mild to moderate muscle atrophy and gait or mobility disturbance. These clinical findings are compatible with our previous study of $CXMD_J$dogs.[14] Representative cross-sectional images of II-2302MA are shown in Figure 2A.

All lower leg muscles of the three $CXMD_J$ showed no change on T1WI and CHESS-T1WI (Fig. 2A, b and d), but almost all lower leg muscles, especially EDL and GC, revealed remarkable hyperintensity on T2WI when compared with the images of normal dogs. We should note that the hyperintensity on TC was rather slight compared with that of the other lower leg muscles (Fig. 2A, f). We found that contrast agent uptake by Gd-T1WI (data not shown) or CHESS-Gd-T1WI (Fig. 2A, h) was increased in the areas where hyperintensity was recorded by T2WI. These findings suggest the necrotic and/or inflammatory changes that were shown in a previous study of *mdx* mice.[21] Hyperintensity was also clearly indicated by CHESS-T2WI in these regions, where hyperintensity on T2WI and contrast agent uptake in Gd-T1WI or CHESS-Gd-T1WI were noted (Fig. 2A, j).

Comparison of MR Signal Intensities of 3-Month-Old Normal and Dystrophic Dogs. To quantitatively evaluate MRI findings of three normal and three $CXMD_J$ dogs, we measured T2 relaxation time, CE based on comparison between SNR of CHESS-T1WI and CHESS-Gd-T1WI, and SNR of CHESS-T2WI. In TC, the T2 relaxation time of $CXMD_J$ dogs was significantly prolonged (49.8 $\pm$ 2.3 ms) when compared with that of normal dogs (39.9 $\pm$ 1.2 ms) ($P = 0.0004$). Moreover, T2 relaxation time of EDL was significantly prolonged in $CXMD_J$ (58.6 $\pm$ 3.1 ms) when compared with not only that in normal dogs (40.0 $\pm$ 0.5 ms) but also that of TC in $CXMD_J$ dogs ($P < 0.0001$ and $P = 0.0008$, respectively) (Fig. 2B, a).

Similarly, the effect of contrast enhancement in TC and EDL of $CXMD_J$ (1.659 $\pm$ 0.077 and 1.936 $\pm$ 0.127-fold) was significantly increased in comparison with that of normal dogs (1.511 $\pm$ 0.009 and 1.528 $\pm$ 0.015 fold) ($P = 0.0413$ and $P = 0.0002$, respectively), but the effect in TC of $CXMD_J$ was more prominent in EDL of $CXMD_J$ ($P = 0.0019$) (Fig. 2B, b).

In TC, the SNR of CHESS-T2WI was significantly increased in $CXMD_J$ (102.3 $\pm$ 12.1) when compared with that of normal dogs (70.0 $\pm$ 3.6) ($P = 0.0019$). Moreover, the SNR of CHESS-T2WI was significantly increased in EDL of $CXMD_J$ (146.0 $\pm$ 11.7) when compared with not only that of normal dogs (69.2 $\pm$ 2.9) but also that in TC of $CXMD_J$ dogs ($P < 0.0001$ and $P = 0.0003$, respectively), indicating EDL was more affected than TC in the early stage of $CXMD_J$ (Fig. 2B, c).

Histopathological Findings in Lower Leg Muscles of 3-month-old Normal and Dystrophic Dogs. To determine the relationship between MRI findings and

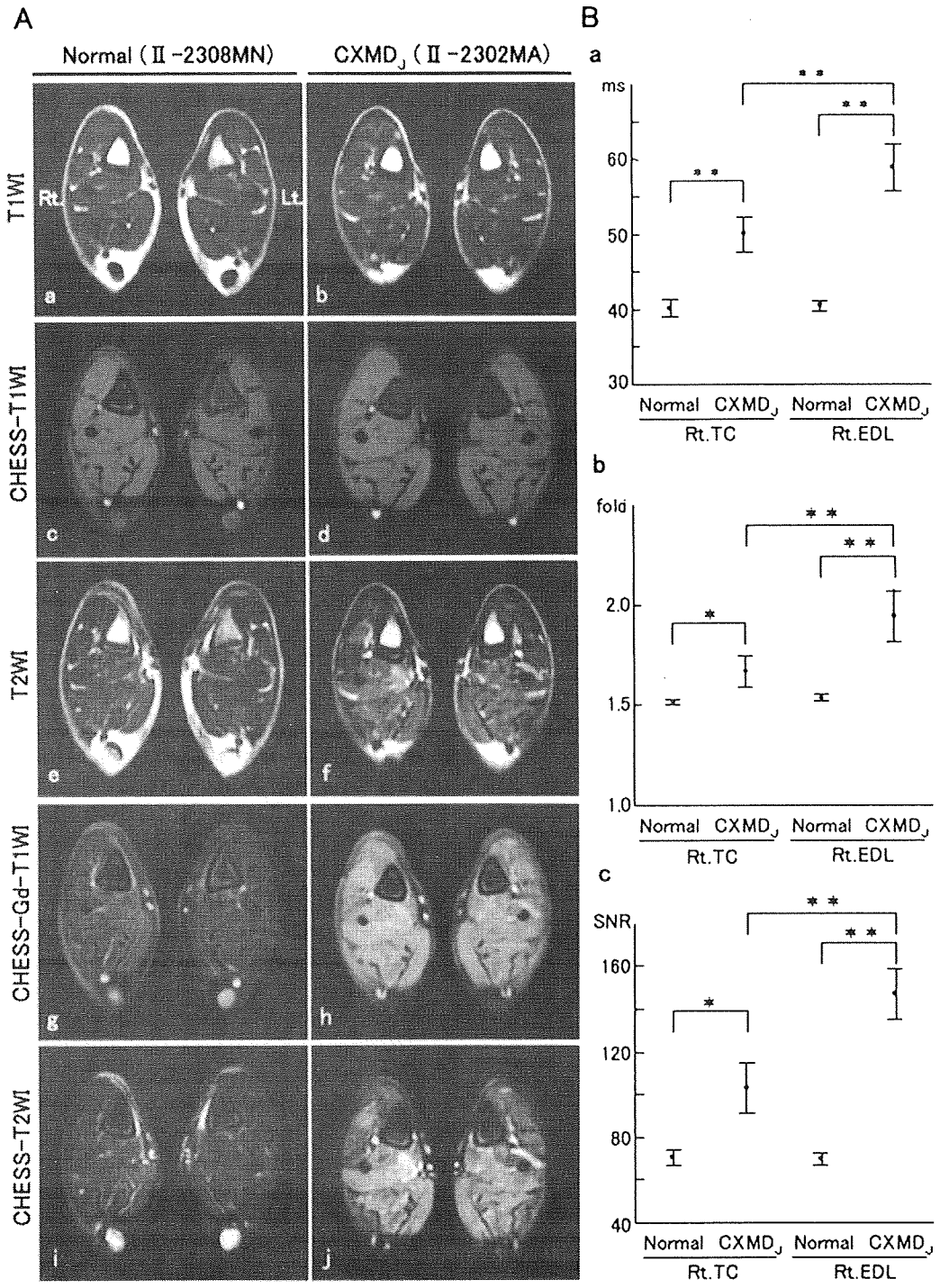

FIGURE 2. Cross-sectional MR images in lower leg muscles of 3-month-old normal and dystrophic dogs and comparison of three quantitative values in Rt. TC and Rt. EDL. **(A)** Representative images of normal (II-2308MN) and dystrophic (II-2302MA) dogs are shown. T1WI **(a, b)**, CHESS-T1WI **(c, d)**, T2WI **(e, f)**, CHESS-Gd-T1WI **(g, h)**, and CHESS-T2WI **(i, j)**. Rt, right side; Lt, left side. **(B)** Comparison of T2 relaxation time **(a)**, contrast enhancement (CE) **(b)**, and SNR of CHESS-T2WI **(c)** between three 3-month-old normal (II-2308MN, II/III-3911MN, and II-4202MN) and three littermate dystrophic (II-2302MA, II/III-3903MA, and II-4204MA) dogs are shown. Rt. TC, right side tibialis cranialis; Rt. EDL, right side extensor digitorum longus. Error bar: mean ± SD; $^*P < 0.05$; $^{**}P < 0.01$.

morphological changes of $CXMD_J$ lower leg muscles, we biopsied the Rt. TC and Rt. EDL of a normal dog (II-2308MN) and a $CXMD_J$ dog (II-2302MA) and carried out histopathological examinations. In TC of the $CXMD_J$, we found necrotic fibers, regenerating myofibers with central nuclei, a slight increase in cellular infiltration, and moderate variation in fiber size (Fig. 3A, c). Immunostaining with anti-IgG antibody, which is a marker for muscle necrosis,[37] revealed a slight degree of IgG uptake in the cytoplasm (Fig. 3A, d). On the other hand, EDL of the $CXMD_J$ showed many necrotic and hypercontracted fibers, severe cellular infiltration, and an increase in interstitial connective tissue (Fig. 3B, c). Moreover, the cytoplasm of this muscle showed a severe degree of IgG uptake (Fig. 3B, d). The necrotic and inflammatory changes in the muscle corresponded to the higher SNR on CHESS-T2W images.

MRI Findings of Lower Leg Muscles in a 7-year-old Normal Dog. Next, we obtained muscle images of a 7-year-old normal dog, 00-174MN (Fig. 4A). As shown in Figure 4A, a, c, e, g, and i, the lower leg muscles showed a homogeneous signal intensity in each sequence. Homogeneous but slight contrast enhancement was found on Gd-T1WI and CHESS-Gd-T1WI, as seen in 3-month-old normal dogs.

MRI Findings of Lower Leg Muscles in 7-Year-Old Dystrophic Dogs. We performed muscle MRI on two 7-year-old $CXMD_J$ dogs. II-C04MA showed muscle weakness and atrophy, gait disturbance, macroglossia, arthrogryposis, and dysphagia, but the dog could still rise and walk. Another dog, II-C12MA, was found to have difficulty in rising at the age of about 6.5 years. These two $CXMD_J$ showed mild clinical symptoms and signs despite their ages, which is sometimes seen in less affected GRMD.[8] We have previously reported that the clinical severity in Beagle-crossed dystrophic dogs was milder than that in GRMD,[14] in accordance with a separate report from another facility.[8]

MRI indicated muscle atrophy in both dogs, but the degree of muscle atrophy was more striking in II-C12MA than that in II-C04MA. Figure 4A, b, d, f, h, and j shows representative cross-sectional images of II-C04MA. On T1WI, almost all lower leg muscles of both dogs, in particular TC, EDL, and GC, revealed diffuse hyperintensity regions (Fig. 4A, b), although FHL and FDL did not show remarkable change compared with the normal dog. On CHESS-T1WI, these hyperintense regions were considerably suppressed, suggesting fat infiltration with progression of the disease (Fig. 4A, d), which was reported in a previous MRI study of DMD.[19]

On T2WI, II-C04MA showed slight and moderate hyperintensity in TC and other lower leg muscles, respectively (Fig. 4A, f). On the other hand, II-C12MA also had an area that showed remarkable T2 hyperintensity with T1 hyperintensity, but there is no area of T2 hyperintensity without T1 hyperintensity, with the exception of FHL (data not shown).

On CHESS-T2WI, FDL, GC, FHL, and FDS of II-C04MA and FHL of II-C12MA showed hyperintensity, but significant signal changes were found in neither TC of II-C04MA nor almost all lower leg muscles of II-C12MA (Fig. 4A, j, and data not shown).

On CHESS-Gd-T1WI of II-C04MA, the CHESS sequence considerably suppressed the hyperintense fat signal, but the contrast agent greatly enhanced the muscle regions left in all lower leg muscles, especially EDL, FHL, FDL, GC, and FDS (Fig. 4A, h). Contrast agent uptake was also found on CHESS-Gd-T1WI of II-C12MA, but the degree of uptake was lower than that of II-C04MA (data not shown).

Comparison of MR Signal Intensity in 7-Year-Old Normal and Dystrophic Dogs. To quantitatively assess the MRI findings of $CXMD_J$ dogs, we calculated the T2 relaxation time, CE, and SNR of CHESS-T2WI in TC of one 7-year-old normal dog and two $CXMD_J$ dogs. T2 relaxation time of TC was moderately prolonged in both $CXMD_J$ dogs (46.4 and 47.4 ms) when compared with that in a normal dog (37.0 ms) (Fig. 4B, a). Similarly, the effect of contrast enhancement was also increased in TC of each $CXMD_J$ (1.439- and 1.465-fold) relative to that of a normal dog (1.229-fold) (Fig. 4B, b). However, the SNR of CHESS-T2WI in TC of both $CXMD_J$ dogs (77.7 and 75.0) was not significantly increased when compared with that of a normal dog (74.7) (Fig. 4B, c). The discrepancy between the SNR of CHESS-T2WI and T2 relaxation times, and the effect of contrast enhancement should be carefully considered in the examination of affected skeletal muscle morphology.

Histopathological Findings in Lower Leg Muscles of 7-year-old Normal and Dystrophic Dogs. To determine the relationship between MRI findings and morphological changes in $CXMD_J$ lower leg muscles, we biopsied the Rt. TC of 00-174MN and

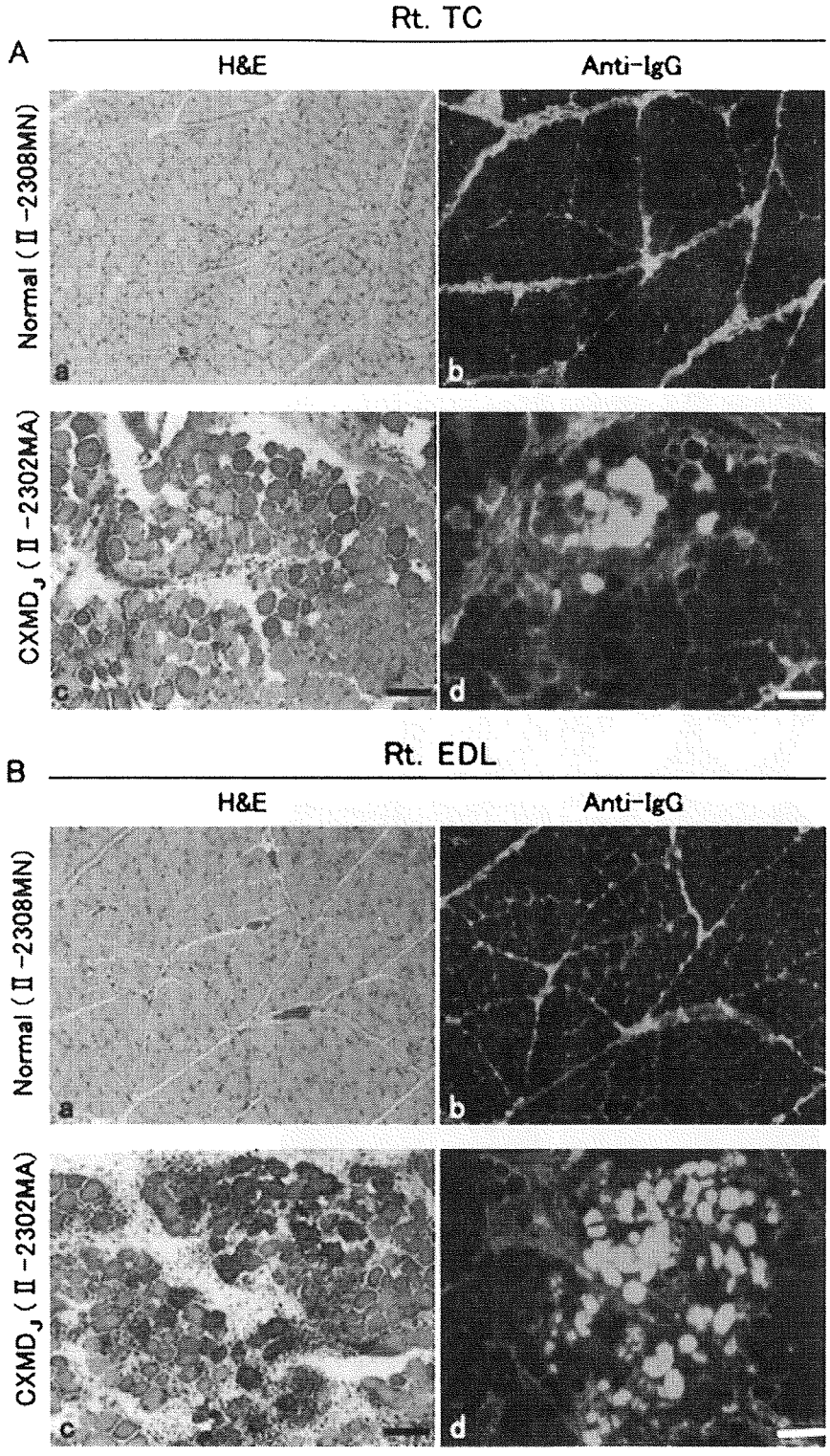

FIGURE 3. Histopathological examinations in Rt. TC and Rt. EDL of 3-month-old normal and dystrophic dogs.**(A)** Hematoxylin and eosin (H&E) staining **(a, c)** and IgG immunostaining **(b, d)** in Rt. TC of 3-month-old normal (II-2308MN) **(a, b)** and dystrophic (II-2302MA) dogs **(c, d)**. **(B)** H&E **(a, c)** and IgG immunostaining **(b, d)** in Rt. EDL of 3-month-old normal (II-2308MN) **(a, b)** and dystrophic (II-2302MA) dogs **(c, d)** are also shown. Bar = 100 μm.

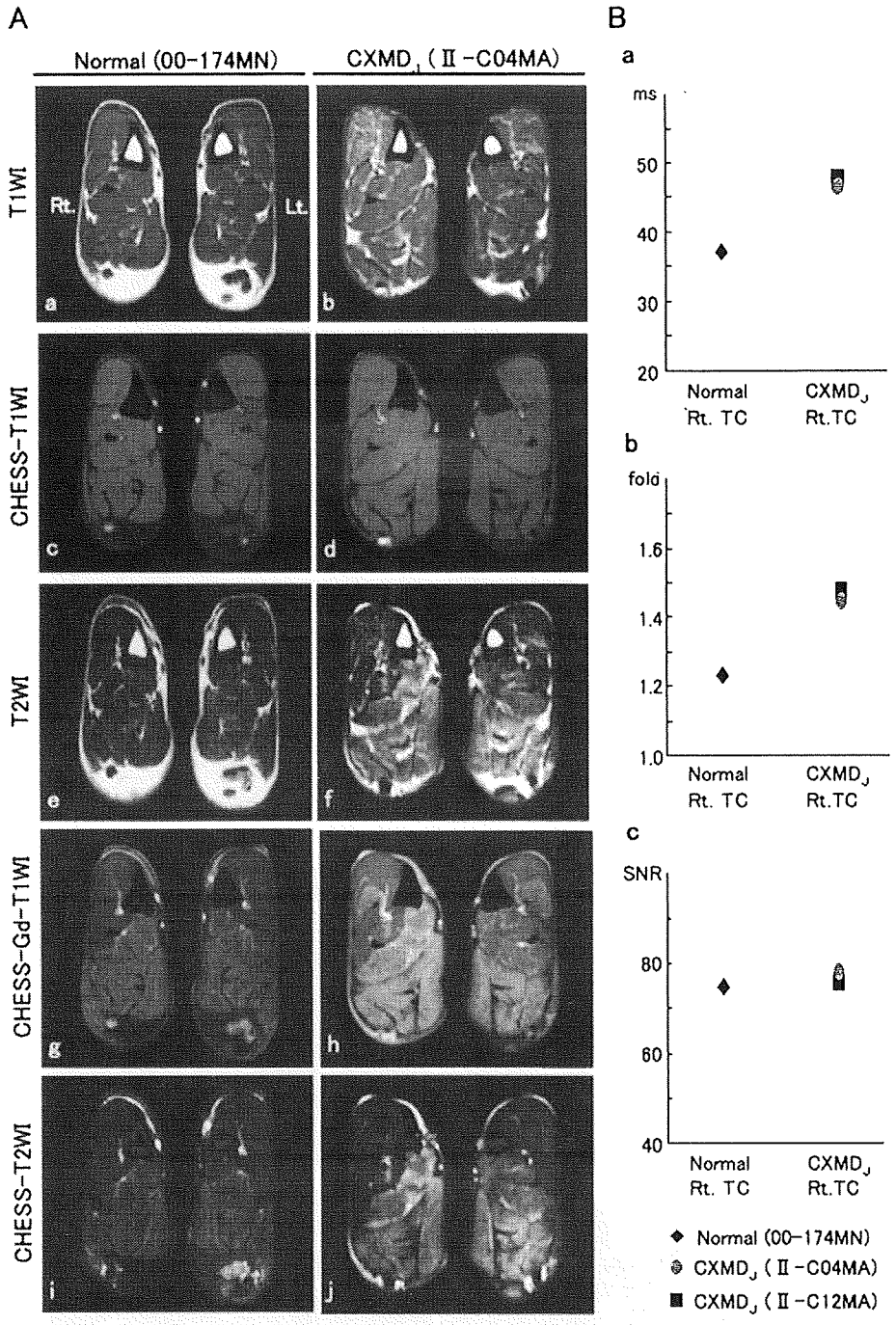

FIGURE 4. Cross-sectional MRI of lower leg muscles of 7-year-old normal and dystrophic dogs and comparison of three quantitative values in Rt. TC. **(A)** Representative images of 7-year-old normal (00-174MN) and dystrophic (II-C04MA) dogs are shown. T1WI **(a, b)**, CHESS-T1WI **(c, d)**, T2WI **(e, f)**, CHESS-Gd-T1WI **(g, h)**, and CHESS-T2WI **(i, j)**. Rt, right side; Lt, left side. **(B)** Comparisons of T2 relaxation time **(a)**, contrast enhancement (CE) **(b)**, and CHESS-T2W SNR **(c)** between the muscles in 7-year-old normal (00-174MN) and dystrophic (II-C04MA and II-C12MA) dogs are shown. TC, tibialis cranialis.

II-C04MA and carried out histopathological examinations. In CXMD$_J$ dogs, we found a few degenerated and many regenerated fibers with central nuclei and a moderate degree of fiber size variation together with fibrotic changes (Fig. 5d). IgG accumulation was found in only a few fibers, but it was extensively distributed in the interstitial tissues (Fig. 5e). Oil red O staining revealed definite fatty infiltration in the CXMD$_J$ dogs (Fig. 5f).

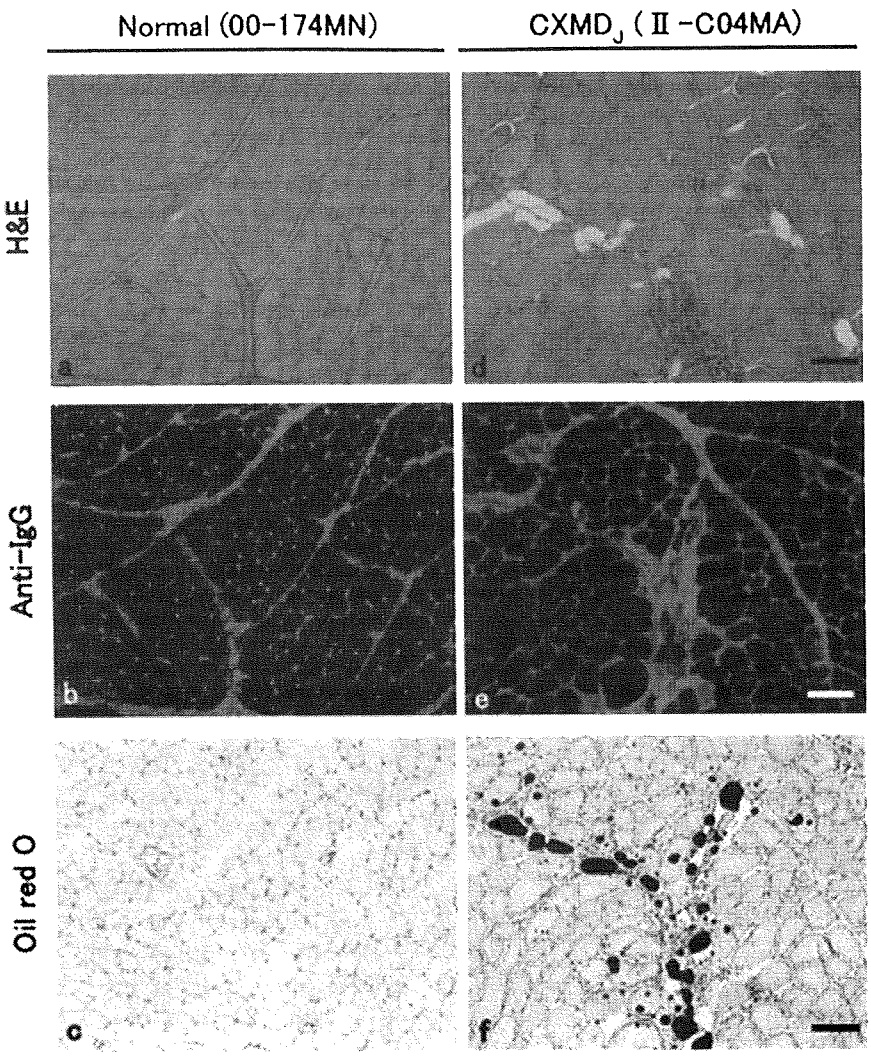

FIGURE 5. Histopathology in Rt. TC of 7-year-old normal and dystrophic dogs. We performed hematoxylin and eosin (H&E) staining **(a, d)**, IgG immunostaining **(b, e)**, and oil red O staining **(c, f)** on tissues of 7-year-old normal (00-174MN) **(a–c)** and dystrophic (II-C04MA) dogs **(d–f)**. Bar = 100 μm.

DISCUSSION

Previous studies have attempted to noninvasively evaluate involvement of striated muscle in DMD patients or the animal models by various MRI sequences; however, a method for more accurate and precise assessment of acute-phase responses such as muscle necrosis and/or inflammation is necessary, because it is difficult to distinguish between these lesions and fat infiltration and/or fibrosis by conventional MRI sequences. Among dystrophic processes, especially in muscle necrosis, the intramuscular water concentration and extracellular components are increased, with the water imbalance having been induced by the deficiency of sarcolemmal membrane integrity.[19,26,38] CHESS-T2WI may be one of the tools to solve this problem, because the sequence can selectively cancel fat tissue signals.

CHESS-T2WI Is Useful to Evaluate Dystrophic Skeletal Muscle Involvement in Early Stage. First, we tried to detect necrotic and/or inflammatory lesions in the early stage of CXMD$_J$ by using a CHESS-T2WI sequence. EDL of a 3-month-old CXMD$_J$ dog showed massive and severe necrosis and inflammatory cell infiltration in the pathological analyses, but TC of the dog revealed localized and moderate necrosis and inflammation. The SNR of CHESS-T2WI in EDL showed a significant increase compared with that in TC. These findings suggest that there is a correlation between SNR of CHESS-T2WI and the degree of necrotic and inflamma-

tory changes in the histopathology. Moreover, the SNR of CHESS-T2WI was consistent with T2 relaxation time or contrast enhancement in the early stage of muscular dystrophy. Previous contrast agent studies sensitively detected early dystrophic muscle involvement that showed the increase of cell membrane permeability.[24,25] In the forelegs of 2-month-old GRMD dogs, the maximum relative enhancement, which was calculated from fat-saturated T1-weighted images pre- and post-gadolinium injection, was almost doubled compared with normal control dogs.[39] However, side effects of the contrast agent itself or cytotoxicity may be of concern, because influx of the contrast agent into damaged muscle fibers occurred. CHESS-T2WI can identify dystrophic lesions without a contrast agent and may facilitate more sensitive and clearer optical evaluation of early dystrophic lesions than other fat suppression sequences, because the SNR on either STIR or the multipoint Dixon technique is lower than that on CHESS.[40]

CHESS-T2WI May Be Able to Differentiate Necrotic and/or Inflammatory Changes from Fatty Changes in Advanced Stage of Dystrophic Dogs. Next, we studied whether CHESS-T2WI is able to evaluate necrotic and/or inflammatory lesions in the advanced stage of $CXMD_J$. TC of 7-year-old $CXMD_J$ dogs showed severe fatty infiltration and an increase in interstitial tissues without necrosis and inflammation. The SNR of CHESS-T2WI in TC was not significantly different from that of the age-matched normal dog, suggesting that CHESS-T2WI is a good tool to evaluate necrotic and/or inflammatory changes, even though extensive fatty infiltration exists. On the other hand, the T2 relaxation time and enhancing effect of the contrast agent were increased, although necrotic and inflammatory changes were not present. It is possible that the prolongation of T2 relaxation time or the increase of contrast enhancement is affected by fatty infiltration, increase of interstitium, and/or microvascular flow, and therefore necrotic and inflammatory changes could be overestimated by these sequences and indexes. CHESS-T2WI may reflect necrotic lesions more precisely in the intermediate to advanced stage without special contrast agents, because the SNR of CHESS-T2WI was elevated in EDL of II-C04MA, where it is thought that necrotic and fatty changes coexist (data not shown). On the other hand, it is also important to evaluate fatty infiltration in the advanced stages of DMD. In a recent study, the percentage of intramuscular fat tissue was measured by three-point Dixon MRI, which may accurately reflect the clinical severity of DMD patients.[41]

Muscle Regeneration in Advanced Stage of $CXMD_J$ May Stabilize Cell Membrane. We found that the majority of muscle fibers in TC of 7-year-old $CXMD_J$ dogs were composed of regenerated fibers with central nuclei, but those fibers did not show IgG uptake, in accordance with the lack of abnormal signals on CHESS-T2WI at this stage. The histopathological findings and muscle physiological functions were ameliorated at the advanced stage in *mdx* mice compared with those in the early stage.[9] Moreover, studies using 31-phosphorus magnetic resonance spectroscopy (^{31}P-MRS) demonstrated biochemical abnormalities in the regulations of intracellular ion and oxidative metabolism of dystrophic muscles at the early stage.[42–45] It was, however, reported that older GRMD (>30 months) did not demonstrate further increases in the inorganic phosphate (Pi) to phosphocreatine (PCr) ratio [Pi/(Pi+PCr)] after exercise, and these results may reflect the relative stabilization of clinical signs and symptoms at the later stage, as far as they were examined by ^{31}P-MRS.[45] Skeletal muscle in the early stage of DMD and the model animals showed enhanced necrotic and regeneration activities due to functionally defective regulation caused by the deficiency of dystrophin. On the other hand, we and others found a lower degree of muscle degeneration at the advanced stage, suggesting some degree of membrane stability remains in regenerated fibers, resulting in resistance to further necrosis. Retention of membrane stability in the advanced stage may be related to the shift of muscle fiber types from fast to slow[46] and/or compensatory expression of utrophin,[47] a homolog of dystrophin.

One of the limitations of the CHESS sequence is that it requires a presaturation pulse. Fat suppression by the CHESS sequence is not applicable with a low magnetic field (<1.5 T), because dispersion of the frequency direction between water and fat depends on the main magnetic field.[48] Another limitation is that CHESS-T2WI does not allow evaluation of fibrotic changes. We, however, suggest that CHESS-T2WI could precisely and perceptively provide much information, such as the presence and severity of necrotic and inflammatory changes throughout all stages of the disease. Moreover, CHESS-T2WI is safer than other conventional sequences, because the sequence does not require

contrast agent enhancement. CHESS-T2WI may be useful to understand the pathological findings, to monitor therapeutic effects in clinical trials, and to predict functional recovery in muscular dystrophies such as DMD.

This study was supported by Health Sciences Research Grants for Research on Psychiatric and Neurological Diseases and Mental Health (H12-kokoro-025, H15-kokoro-021, H18-kokoro-019), Human Genome and Gene Therapy (H13-genome-001, H16-genome-003), and Health and Labor Sciences Research Grants for Translation Research (H19-translational research-003) from the Ministry of Health, Labor and Welfare of Japan, and Grants-in-Aid for Scientific Research from the Ministry of Education, Science, Sports and Culture of Japan (to S.T.). The authors thank Hideki Kita, Shin'ichi Ichikawa, Yumiko Yahata, Takayuki Nakayama, Masayoshi Sawada, and Kazue Kinoshita (JAC, Inc., Tokyo) for maintenance of the dogs, and Ryoko Nakagawa and Satoru Masuda (Department of Molecular Therapy, National Institute of Neuroscience, NCNP, Tokyo) for their technical assistance. We also thank Dr. Hironaka Igarashi (Center for Integrated Human Brain Science, Niigata University) for technical advice concerning MRI.

REFERENCES

1. Moser H. Duchenne muscular dystrophy: pathogenetic aspects and genetic prevention. Hum Genet 1984;66: 17–40.
2. Koenig M, Hoffman EP, Bertelson CJ, Monaco AP, Feener C, Kunkel LM. Complete cloning of the Duchenne muscular dystrophy (DMD) cDNA and preliminary genomic organization of the DMD gene in normal and affected individuals. Cell 1987;50:509–517.
3. Campbell KP. Three muscular dystrophies: loss of cytoskeleton–extracellular matrix linkage. Cell 1995;80:675–679.
4. Ervasti JM, Ohlendieck K, Kahl SD, Gaver MG, Campbell KP. Deficiency of a glycoprotein component of the dystrophin complex in dystrophic muscle. Nature 1990;345:315–319.
5. Cullen MJ, Mastaglia FL. Morphological changes in dystrophic muscle. Br Med Bull 1980;36:145–152.
6. Marden FA, Connolly AM, Siegel MJ, Rubin DA. Compositional analysis of muscle in boys with Duchenne muscular dystrophy using MR imaging. Skel Radiol 2005;34:140–148.
7. Coulton GR, Morgan JE, Partridge TA, Sloper JC. The mdx mouse skeletal muscle myopathy: I. A histological, morphometric and biochemical investigation. Neuropathol Appl Neurobiol 1988;14:53–70.
8. Valentine BA, Cooper BJ, de Lahunta A, O'Quinn R, Blue JT. Canine X-linked muscular dystrophy. An animal model of Duchenne muscular dystrophy: clinical studies. J Neurol Sci 1988;88:69–81.
9. Muntoni F, Mateddu A, Marchei F, Clerk A, Serra G. Muscular weakness in the mdx mouse. J Neurol Sci 1993;120: 71–77.
10. Tanabe Y, Esaki K, Nomura T. Skeletal muscle pathology in X chromosome-linked muscular dystrophy (mdx) mouse. Acta Neuropathol (Berl) 1986;69:91–95.
11. Cooper BJ, Winand NJ, Stedman H, Valentine BA, Hoffman EP, Kunkel LM, et al. The homologue of the Duchenne locus is defective in X-linked muscular dystrophy of dogs. Nature 1988;334:154–156.
12. Valentine BA, Cooper BJ, Cummings JF, de Lahunta A. Canine X-linked muscular dystrophy: morphologic lesions. J Neurol Sci 1990;97:1–23.
13. Shimatsu Y, Katagiri K, Furuta T, Nakura M, Tanioka Y, Yuasa K, et al. Canine X-linked muscular dystrophy in Japan (CXMDJ). Exp Anim 2003;52:93–97.
14. Shimatsu Y, Yoshimura M, Yuasa K, Urasawa N, Tomohiro M, Nakura M, et al. Major clinical and histopathological characteristics of canine X-linked muscular dystrophy in Japan, CXMDJ. Acta Myol 2005;24:145–154.
15. Yugeta N, Urasawa N, Fujii Y, Yoshimura M, Yuasa K, Wada MR, et al. Cardiac involvement in beagle-based canine X-linked muscular dystrophy in Japan (CXMDJ): electrocardiographic, echocardiographic, and morphologic studies. BMC Cardiovasc Disord 2006;6:47.
16. Liu M, Chino N, Ishihara T. Muscle damage progression in Duchenne muscular dystrophy evaluated by a new quantitative computed tomography method. Arch Phys Med Rehabil 1993;74:507–514.
17. Shimizu J, Matsumura K, Kawai M, Kunimoto M, Nakano I. X-ray CT of Duchenne muscular dystrophy skeletal muscles—chronological study for five years [in Japanese]. Rinsho Shinkeigaku 1991;31:953–959.
18. Mercuri E, Pichiecchio A, Allsop J, Messina S, Pane M, Muntoni F. Muscle MRI in inherited neuromuscular disorders: past, present, and future. J Magn Reson Imaging 2007;25: 433–440.
19. Huang Y, Majumdar S, Genant HK, Chan WP, Sharma KR, Yu P, et al. Quantitative MR relaxometry study of muscle composition and function in Duchenne muscular dystrophy. J Magn Reson Imaging 1994;4:59–64.
20. Schreiber A, Smith WL, Ionasescu V, Zellweger H, Franken EA, Dunn V, et al. Magnetic resonance imaging of children with Duchenne muscular dystrophy. Pediatr Radiol 1987;17:495–497.
21. McIntosh LM, Baker RE, Anderson JE. Magnetic resonance imaging of regenerating and dystrophic mouse muscle. Biochem Cell Biol 1998;76:532–541.
22. Matsumura K, Nakano I, Fukuda N, Ikehira H, Tateno Y, Aoki Y. Proton spin-lattice relaxation time of Duchenne dystrophy skeletal muscle by magnetic resonance imaging. Muscle Nerve 1988;11:97–102.
23. Dunn JF, Zaim-Wadghiri Y. Quantitative magnetic resonance imaging of the mdx mouse model of Duchenne muscular dystrophy. Muscle Nerve 1999;22:1367–1371.
24. Amthor H, Egelhof T, McKinnell I, Ladd ME, Janssen I, Weber J, et al. Albumin targeting of damaged muscle fibres in the mdx mouse can be monitored by MRI. Neuromuscul Disord 2004;14:791–796.
25. Straub V, Donahue KM, Allamand V, Davisson RL, Kim YR, Campbell KP. Contrast agent-enhanced magnetic resonance imaging of skeletal muscle damage in animal models of muscular dystrophy. Magn Reson Med 2000;44:655–659.
26. Walter G, Cordier L, Bloy D, Sweeney HL. Noninvasive monitoring of gene correction in dystrophic muscle. Magn Reson Med 2005;54:1369–1376.
27. Burstein D, Taratuta E, Manning WJ. Factors in myocardial "perfusion" imaging with ultrafast MRI and Gd-DTPA administration. Magn Reson Med 1991;20:299–305.
28. Baxter AB, Lazarus SC, Brasch RC. In vitro histamine release induced by magnetic resonance imaging and iodinated contrast media. Invest Radiol 1993;28:308–312.
29. Nomura M, Takeshita G, Katada K, Nakamura M, Kizukuri T, Ogura Y, et al. A case of anaphylactic shock following the administration of Gd-DTPA [in Japanese]. Nippon Igaku Hoshasen Gakkai Zasshi 1993;53:1387–1391.
30. Krinsky G, Rofsky NM, Weinreb JC. Nonspecificity of short time inversion recovery (STIR) as a technique of fat suppression: pitfalls in image interpretation. AJR Am J Roentgenol 1996;166:523–526.
31. Scarabino T, Giannatempo GM, Popolizio T, Scarale MG, Cammisa M, Salvolini U. Fast spin echo imaging of vertebral metastasis: comparison of fat suppression techniques (FSE-CHESS, STIR-FSE) [in Italian]. Radiol Med (Torino) 1996; 92:180–185.
32. Drevelegas A, Pilavaki M, Chourmouzi D. Lipomatous tumors of soft tissue: MR appearance with histological correlation. Eur J Radiol 2004;50:257–267.

33. Galant J, Marti-Bonmati L, Saez F, Soler R, Alcala-Santaella R, Navarro M. The value of fat-suppressed T2 or STIR sequences in distinguishing lipoma from well-differentiated liposarcoma. Eur Radiol 2003;13:337–343.
34. Morimoto Y, Tanaka T, Masumi S, Tominaga K, Shibuya T, Kito S, et al. Significance of frequency-selective fat saturation T2-weighted MR images for the detection of bone marrow edema in the mandibular condyle. Cranio 2004;22:115–123.
35. Cook LL, Foster PJ, Karlik SJ. Pathology-guided MR analysis of acute and chronic experimental allergic encephalomyelitis spinal cord lesions at 1.5T. J Magn Reson Imaging 2005; 22:180–188.
36. Bonny JM, Zanca M, Boespflug-Tanguy O, Dedieu V, Joandel S, Renou JP. Characterization in vivo of muscle fiber types by magnetic resonance imaging. Magn Reson Imaging 1998;16:167–173.
37. Straub V, Rafael JA, Chamberlain JS, Campbell KP. Animal models for muscular dystrophy show different patterns of sarcolemmal disruption. J Cell Biol 1997;139:375–385.
38. Mattila KT, Lukka R, Hurme T, Komu M, Alanen A, Kalimo H. Magnetic resonance imaging and magnetization transfer in experimental myonecrosis in the rat. Magn Reson Med 1995;33:185–192.
39. Thibaud JL, Monnet A, Bertoldi D, Barthelemy I, Blot S, Carlier PG. Characterization of dystrophic muscle in golden retriever muscular dystrophy dogs by nuclear magnetic resonance imaging. Neuromuscul Disord 2007;17:575–584.
40. Mao J, Yan H, Brey WW, Bidgood WD Jr, Steinbach JJ, Mancuso A. Fat tissue and fat suppression. Magn Reson Imaging 1993;11:385–393.
41. Wren TA, Bluml S, Tseng-Ong L, Gilsanz V. Three-point technique of fat quantification of muscle tissue as a marker of disease progression in Duchenne muscular dystrophy: preliminary study. AJR Am J Roentgenol 2008;190:W8–12.
42. Dunn JF, Tracey I, Radda GK. A 31P-NMR study of muscle exercise metabolism in mdx mice: evidence for abnormal pH regulation. J Neurol Sci 1992;113:108–113.
43. Dunn JF, Tracey I, Radda GK. Exercise metabolism in Duchenne muscular dystrophy: a biochemical and [31P]-nuclear magnetic resonance study of mdx mice. Proc Biol Sci 1993; 251:201–206.
44. Le Rumeur E, Le Tallec N, Lewa CJ, Ravalec X, de Certaines JD. In vivo evidence of abnormal mechanical and oxidative functions in the exercised muscle of dystrophic hamsters by 31P-NMR. J Neurol Sci 1995;133:16–23.
45. McCully K, Giger U, Argov Z, Valentine B, Cooper B, Chance B, et al. Canine X-linked muscular dystrophy studied with in vivo phosphorus magnetic resonance spectroscopy. Muscle Nerve 1991;14:1091–1098.
46. Yuasa K, Nakamura A, Hijikata T, Takeda S. Dystrophin deficiency in canine X-linked muscular dystrophy in Japan (CXMDJ) alters myosin heavy chain expression profiles in the diaphragm more markedly than in the tibialis cranialis muscle. BMC Musculoskel Disord 2008;9:1.
47. Hirst RC, McCullagh KJ, Davies KE. Utrophin upregulation in Duchenne muscular dystrophy. Acta Myol 2005;24: 209–216.
48. Haase A, Frahm J, Hanicke W, Matthaei D. 1H NMR chemical shift selective (CHESS) imaging. Phys Med Biol 1985;30: 341–344.

Neuropathology 2009; **29**, 494–501 doi:10.1111/j.1440-1789.2009.01028.x

Symposium: Clinicopathological aspects of neuromuscular disorders – A new horizon

Exon-skipping therapy for Duchenne muscular dystrophy

Akinori Nakamura and Shin'ichi Takeda

Department of Molecular Therapy, National Institute of Neuroscience, National Center of Neurology and Psychiatry (NCNP), Ogawa-higashi, Kodaira, Tokyo, Japan

Duchenne muscular dystrophy (DMD) is a lethal muscle disorder caused by mutations in the *DMD* gene for which no mutation-targeted therapy has been available thus far. However, exon-skipping mediated by antisense oligonucleotides (AOs), which are short single-strand DNAs, has considerable potential for DMD therapy, and clinical trials in DMD patients are currently underway. This exon-skipping therapy changes an out-of-frame mutation into an in-frame mutation, aiming at conversion of a severe DMD phenotype into a mild phenotype by restoration of truncated dystrophin expression. Recently, stable and less-toxic AOs have been developed, and their higher efficacy was confirmed in mice and dog models of DMD. In this review, we briefly summarize the genetic basis of DMD and the potential and perspectives of exon skipping as a promising therapy for this disease.

Key words: antisense oligonucleotide, DMD animal model, *DMD* gene, Duchenne muscular dystrophy (DMD), dystrophin, exon skipping.

INTRODUCTION

Muscular dystrophy is a group of disorders that shows progressive muscle atrophy and weakness and the histopathology of which reveals degeneration and regeneration of muscle fibers. Among them, Duchenne muscular dystrophy (DMD), an X-linked disorder, is the most common and produces the most severe phenotype. This disorder manifests around the age 2–5 years by difficulty in walking, and the skeletal muscle involvement is progressive, resulting in patients being wheelchair-bound by the age of 13. The patients die of cardiac or respiratory failure due to dilated cardiomyopathy around the age of 30 years, at least in Japan. The responsible gene, *DMD*, encodes dystrophin, which is expressed at the sarcolemma of muscle fibers, and *DMD* mutations interrupt the reading-frame, resulting in a complete loss of dystrophin expression, which causes DMD.[1] The histopathology shows degeneration, necrosis, inflammatory cell invasion, and regeneration of muscle fibers, which are eventually replaced by fibrous connective and fat tissue. Besides DMD, two phenotypes of the dystrophin-deficient condition, Becker muscular dystrophy (BMD) and X-linked dilated cardiomyopathy (XLDCM) are known. BMD is a milder variant of DMD, and XLDCM shows dilated cardiomyopathy without overt skeletal muscle signs and symptoms. All three phenotypes of dystrophin deficiency are called dystrophinopathies.

Several therapeutic strategies for treatment of DMD have been investigated extensively: gene therapy using micro-dystrophin with an adeno-associated virus (AAV) vector,[2] stem cell transplantation using muscle satellite cells[3] or bone marrow stromal cells,[4] and read-through therapy for nonsense mutations.[5] However, an effective treatment has not yet been established. In recent years, exon skipping using antisense oligonucleotides (AOs) has been considered one of the therapeutic strategies for restoration of dystrophin expression at the sarcolemma. AOs are artificial nucleic acids that recognize a specific sequence of the mRNA, resulting in a change in the splicing pattern or translation. Currently, various AOs possessing the properties of high stability, high efficacy and low toxicity, have been developed. Here, we review advances in exon-skipping therapy for DMD.

THE *DMD* GENE AND ITS MUTATION

The *DMD* gene is located on the human chromosome Xp2.1, and it is the largest gene in the human genome, with

Correspondence: Shin'ichi Takeda, MD, PhD, Department of Molecular Therapy, National Institute of Neuroscience, National Center of Neurology and Psychiatry (NCNP), 4-1-1 Ogawa-higashi, Kodaira, Tokyo 187-8502, Japan. Email: takeda@ncnp.go.jp

Received 30 January 2009 and accepted 22 March 2009; published online 22 May 2009.

79 exons spanning more than 2500 kb. The *DMD* gene encodes a product called dystrophin. Full-length dystrophin mRNA is about 14 kb and is mainly expressed in skeletal, cardiac and smooth muscles, and the brain. Dystrophin is a rod-shape structure that consists of four domains: (i) the N-terminal actin-binding domain; (ii) a rod domain composed of 24 spectrin-like rod repeats and 4 hinges; (iii) a cysteine-rich domain that interacts with dystroglycan and sarcoglycan complexes; and (iv) the C-terminal domain that interacts with the syntrophin complex and dystrobrevin. Dystrophin is localized at the sarcolemma and forms a dystrophin-glycoprotein complex (DGC) with dystroglycan, sarcoglycan, and syntrophin/dystrobrevin complexes. Then, DGC links the cytoskeletal protein actin to the basal lamina of muscle fibers. DGC is considered to work as a membrane stabilizer during muscle contraction or a transducer of signals from the extracellular matrix to the muscle cytoplasm via its interactions with intracellular signaling molecules.[6] Dystrophin deficiency leads to a condition in which the membrane is leaky under mechanical or hypo-osmotic stress. Consequently, Ca^{2+} permeability is increased, and various Ca^{2+}-dependent proteases, such as calpain, are activated in dystrophin deficiency. It has also been proposed that alteration of the expression or function of the plasma membrane proteins associated with dystrophin, such as neuronal nitric oxide synthase (nNOS), aquaporin-4, Na^+ channel, L-type Ca^{2+} channel, and stretch-activated channel, are involved in the molecular mechanisms of muscle degeneration.[6]

In DMD patients, various mutations in the *DMD* gene, such as missense, nonsense, deletion, insertion, or duplication, have been identified (http://www.hgmd.org). In general, when the reading-frame of amino acids is disrupted by a mutation (out-of-frame), dystrophin is not expressed, resulting in the severe phenotype of DMD. On the other hand, when the reading-frame is maintained despite the existence of a mutation (in-frame), a truncated but still functional dystrophin is expressed, leading to the more benign phenotype of Becker muscular dystrophy (BMD). Ninety-two percent of the DMD/BMD phenotypes are explained by the "frame-shift theory." In the *DMD* gene, there are two hot spots for mutation: around exons 3–7 and exons 45–55.

RATIONALE OF EXON-SKIPPING THERAPY IN DMD

In DMD, dystrophin is basically absent at the sarcolemma, although some dystrophin-positive fibers, which are called revertant fibers, are detected in DMD patients and DMD animal models. The number of revertant fibers increases with age due to the cycle of degeneration and regeneration.[7,8] It is currently thought that the molecular mechanism underlying revertant fibers is the skipping of exon(s) around the original mutation, which gives rise to correction of the reading frame and expression of dystrophin at the sarcolemma.[9] Consequently, exon skipping has attracted attention as a strategy for restoration of dystrophin expression in DMD.[8–10] In addition, exon-skipping therapy for DMD has been advanced by the development of several new AOs.[11] Exon-skipping therapy has been reported to be practical for up to 90% of DMD patients having a deletion mutation.[12,13] In addition, the ethical issues involved in exon-skipping therapy are fewer in number than those in gene therapy or stem-cell transplantation therapy because AOs are classified as a drug rather than a gene therapy agent by the Food and Drug Administration (FDA) of the USA and representative agencies in the EU and Japan. Based on reports that asymptomatic patients with high blood creatine kinase concentrations have an in-frame deletion in the *DMD* gene,[14,15] it is possible that exon-skipping therapy could convert DMD phenotype to an asymptomatic phenotype rather than the milder phenotype of dystrophin deficiency, BMD.

DEVELOPMENT OF ANTISENSE OLIGONUCLEOTIDE AND DESIGN OF SEQUENCE

Antisense oligonucleotides are chemically synthesized 20–25 base-long single-strand DNAs that are designed to hybridize with a complementary sequence in the target mRNA. In 1989, Isis Pharmaceuticals developed the AO drug Vitravene (fomivirsen) for retinitis due to cytomegalovirus infection in AIDS patients, and it was the first AO approved by the FDA. However, the clinical application did not go smoothly because of adverse effects such as inflammation, and it was terminated in 1999.

Various chemistries for AOs have been proposed to overcome the unstable nature of single-strand DNA or RNA molecules (Fig. 1). Several modifications of AOs include a bicyclic-locked nucleic acid (LNA), peptide nucleic acid (PNA), ethylene-bridged nucleic acid (ENA), 2′-O-methyl phosphorothionate AO (2OMeAO), phosphorodiamidate morpholino oligomer (PMO: morpholino), and peptide-linked PMO (PPMO).[16,17] Development of appropriate AOs requires consideration of several characteristics of AOs, such as the chemical specificity, affinity, nuclease resistance, stability, safety, and ease of synthesis,[16,18] but among them, 2OMeAO and PMO are the most frequently utilized because of their suitable properties.

The structure of 2OMeAO is similar to that of RNA, but it has been methylated at the 2′-OH position of the ribose ring. 2OMeAO is widely used because it is relatively cheap to produce and easy to synthesize, has high stability and

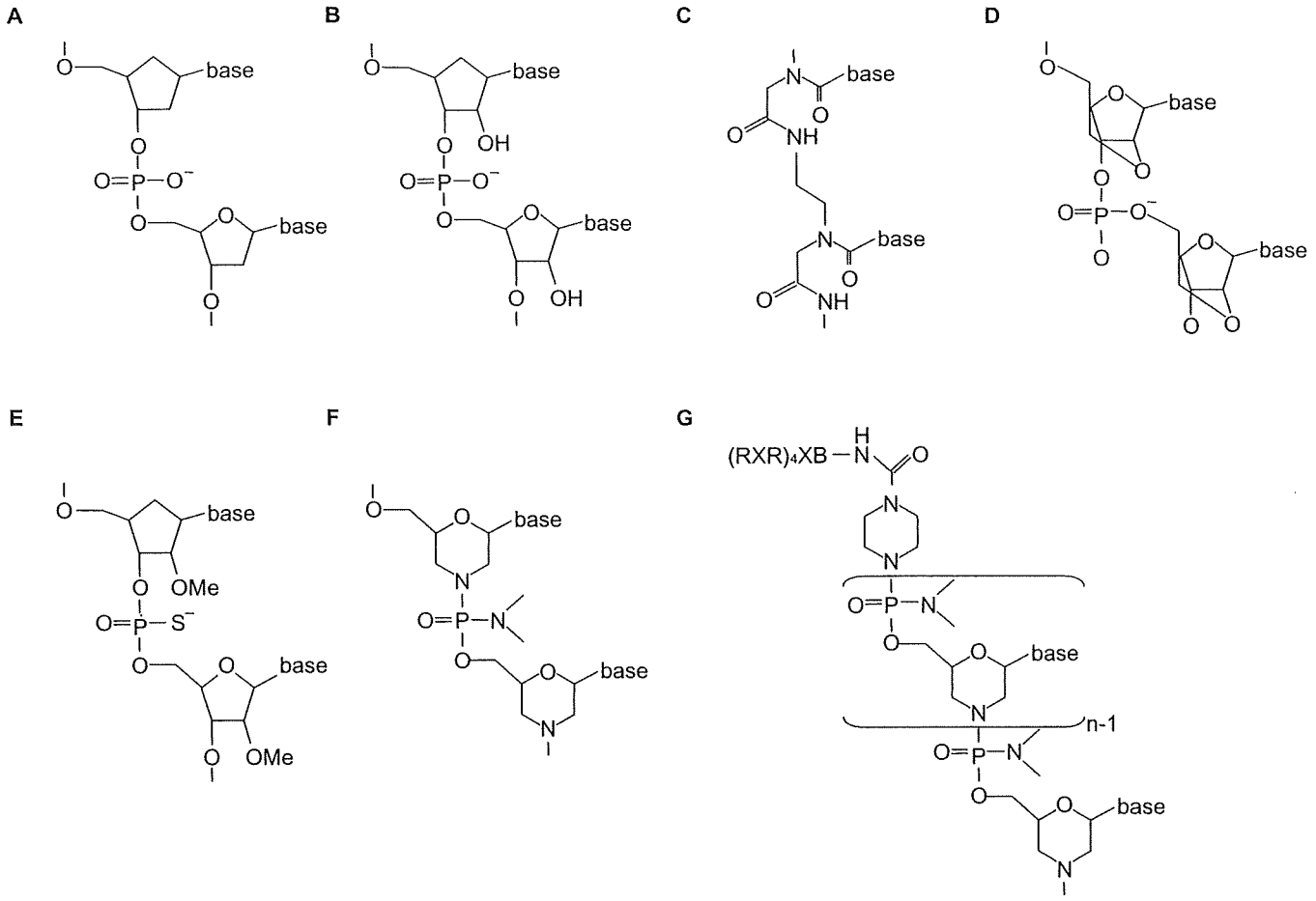

Fig. 1 Chemistries used for exon skipping. A, DNA; B, RNA; C, peptide nucleic acid (PNA); D, ethylene-bridged nucleic acid (ENA); E, 2′-O-methyl phosphorothionate antisense oligonucleotide (2OMeAO); F, phosphorodiamidate morpholino oligomer (PMO) (morpholino), G, peptide-linked PMO (PPMO).

affinity to mRNA, and is also resistant to nucleases. However, the low solubility of 2OMeAO prevents its use at higher dosages.[19]

PMO has a morpholine ring instead of a deoxyribose ring in DNA or ribose ring in RNA, and the morpholine rings bind to each other through phosphorodiamidate instead of phosphoric acid. PMO is non-ionic, which minimizes protein interactions and nonspecific antisense effects, and it has several advantages such as high solubility in water and high binding capacity to mRNA. PMO does not stimulate or activate either Toll-like receptors or inflammatory responses mediated by interferon or NF-κB. AVI Biopharma Inc. (Corvallis, OR, US), which is the only pharmaceutical company that currently produces a Good Manufacturing Practice grade of PMO, has promoted several clinical trials targeting cardiovascular restenosis (Phase II, finished), hepatitis C virus (Phase I, finished), Ebola virus (Phase I, ongoing), Marburg virus (Phase I, ongoing), and rheumatoid arthritis (Phase I, ongoing). To improve the stability of PMO in blood and cells and to increase the uptake of PMO into the cells, cell-penetrating peptides (CPPs) such as β-alanine (B), β-arginine (R), or 6-aminohexane (X) are added, and the compound is called a peptide-conjugated PMO (PPMO).

Designing the sequence of an AO to skip a particular exon in the splicing process from premature mRNA to mRNA is very important.[16,20] Knowledge of the molecular mechanism of splicing tells us that some proteins and splicesome complexes are involved in the splicing machinery through an exon-intron consensus sequence or an exon splicing enhancer (ESE). AOs target the exon-intron boundaries or the ESE and subsequently can inhibit the binding of the spliceosome to premature mRNA. However, when web-based software, such as ESEfinder (http://rulai.cshl.edu/tools/ESE), is used to design an AO sequence to target an ESE, exon-skipping is not always induced.[21,22] An AO targeting a non-ESE sequence such as exon-intron boundary sequences can often effectively induce exon skipping, but the effects of the same AO differ *in vitro* and may also differ *in vivo*. Recently, Wee *et al.*

developed bioinformatics tools to optimize AO sequences based on the pre-mRNA secondary structure.[23]

EXON SKIPPING IN DMD ANIMAL MODELS

Before application of AOs to exon skipping in DMD, *in vitro* and *in vivo* studies using animal models are indispensable. Cultured skeletal muscle cells derived from DMD patients are often used to evaluate exon-skipping efficiency.[24,25] However, *in vitro* studies are limited because while we can examine the effectiveness of skipping itself, we cannot evaluate the functional repair in an *in vitro* system. On the other hand, animal models can be used to assess the efficacy of exon skipping as well as the improvement of muscle function. In this section, studies of the DMD mouse models *mdx* and *mdx*52, which we established, and dystrophic dog will be described.

Mdx mouse

The *mdx* mouse has a nonsense mutation in exon 23 of the *DMD* gene, resulting in loss of dystrophin. This mouse shows a mild but non-progressive muscle weakness of the limbs, although progressive muscle degeneration, necrosis and fibrosis occur in respiratory muscles including the diaphragm.[26] Lu *et al.* reported the local administration of 2OMeAO with the non-ionic polymer F127, which promotes intracellular uptake of 2OMeAO, to the skeletal muscles of 2-week-old *mdx* mice. The result showed that dystrophin together with β-dystroglycan, sarcoglycans, and nNOS was restored in 20% of the muscle fibers.[22] Furthermore, systemic administration of the anti-sequences of the same 2OMeAO with F127 revealed that dystrophin was expressed in the skeletal muscle of the whole body except the heart. There was no toxicity of 2OMeAO, but the expression did not reach a therapeutic level.[22] Wells *et al.* reported that local administration of 2OMeAO using electroporation restored dystrophin expression to up to 20% of the normal level.[27] Systemic induction of dystrophin expression by PMO administration has reached a feasible level in whole body skeletal muscle, although not the heart.[20,28] In addition, the more recently developed PPMO induced high expression of dystrophin in the heart as well in whole body skeletal muscles.[29] A unique exon-skipping method was proposed in which the mutated exon 23 on the mRNA of *mdx* mice is removed by a single administration of an AAV vector expressing antisense sequences linked to a modified U7 small nuclear RNA.[30] This may teach us a method to prevent repeated injections of AO. Goyenvalle *et al.* indeed showed a strong and long-term recovery of dystrophin expression and improvement of muscle function in *mdx* mice,[30] but the issue of the cytotoxicity of AAV vectors and finding a way to prevent immune responses due to subsequent injections of AAV vectors needs to be addressed.

Dystrophic dog

Muscular dystrophy in dogs was originally identified in golden retrievers and designated "Golden retriever muscular dystrophy" (GRMD). GRMD shows progressive skeletal muscle weakness and atrophy as well as abnormal electrocardiographic findings and myocardial fibrosis, like those seen in DMD. However, the dogs are too large to be maintained conveniently, so we have established a colony of medium-sized beagle-based dystrophic dogs (canine X-linked muscular dystrophy in Japan: $CXMD_J$) at the National Center of Neurology and Psychiatry, Tokyo, by using artificial insemination of frozen GRMD semen.[31] The level of serum creatine kinase in $CXMD_J$ is very high soon after birth, and about 25–33% of the pups die of respiratory failure during the neonatal period. Around the age of 2–3 months, atrophy and weakness of limb muscles appear, then the dogs develop gait disturbance, joint contracture, macroglossia, and dysphasia. Those symptoms rapidly progress until the dogs are 10 months of age, and then the progression is retarded.[32] $CXMD_J$, GRMD, and DMD have similar cardiac involvement, including distinct deep Q-waves on the electrocardiogram and fibrosis of the left ventricular wall.[33] The distinct deep Q-waves are ascribed to fibrosis in the posterobasal region of the left ventricular wall in DMD, but we found that the deep Q-waves on echocardiograms precede the development of histopathologically apparent fibrosis in $CXMD_J$.[33] When we investigated the cardiac pathology of $CXMD_J$, we found that the Purkinje fibers showed remarkable vacuolar degeneration despite the absence of detectable fibrotic lesions in the ventricular myocardium. The degenerated Purkinje fibers were coincident with overexpression of Dp71, a C-terminal truncated isoform of dystrophin, at the sarcolemma and translocation of calcium-dependent protease μ-calpain to the cell periphery near the sarcolemma or in the vacuoles. Utrophin, a homologue of dystrophin, was highly upregulated in the Purkinje fibers in the early stage, but the expression was dislocated when vacuolar degeneration was recognized at 4 months of age.[34] The selective degeneration of Purkinje fibers can be associated with distinct deep Q-waves on electrocardiograms and the fatal arrhythmia seen in dystrophinopathy. Thus, the dystrophic dog is a useful model to examine pathogenesis and therapeutic strategies because the phenotype and genetic background are closer to human DMD than those of the mouse model.

The dystrophic dogs have a point mutation at the intron 6 splice acceptor site in the canine *DMD* gene, resulting in skipping of exon 7. A premature stop codon arises in exon

8 and dystrophin is not produced. Recently, we and researchers at the Children's National Medical Center in the USA used three PMOs targeting exons 6 and 8 to convert an out-of-frame mutation into an in-frame mutation, and mixtures of the PMO were systemically administered to CXMD$_J$.[35] The result showed that dystrophin was restored in the entire body skeletal muscle except the heart but that heart muscle function was improved. Thus, we showed for the first time that multi exon-skipping is feasible *in vivo*. Another study reported that PPMO had the highest efficacy in restoration of dystrophin expression when the effectiveness of exon skipping of 2OMeAO, PMO, and PPMO was compared in GRMD muscle cells.[36]

*Mdx*52 mouse

Katsuki and his colleagues generated another DMD mouse model, *mdx*52, in which exon 52 of the murine *DMD* gene was deleted by using a homologous recombination technique.[37] Like the *mdx* mouse, *mdx*52 lacks dystrophin and presents dystrophic changes including muscle hypertrophy. In particular, the retina-specific dystrophin isoform Dp260 is absent and abnormal electroretinographic findings were detected.[38] Recently, we tried exon 51-skipping using PMO in *mdx*52 mice to convert an out-of-frame mutation into an in-frame mutation and found restoration of dystrophin expression in various muscles and improvement of muscle pathology and function (Aoki *et al.*, unpublished data).

PROSPECTS FOR CLINICAL TRIALS FOR DMD

It is thought that the number of patients having the same nonsense or deletion mutation of exon 23 as the *mdx* mouse or the same deletion of exon 7 as the dystrophic dog is very small. To provide exon-skipping therapy to more patients, it will be necessary to target the hot spots of mutation in the *DMD* gene. Among the mutation hot spots, patients having one and more deletions within exons 45–55 account for 60% of DMD patients having deletion mutations, making this area a prominent target. This section reviews the preclinical studies of exon skipping targeting one exon (single-exon skipping) and multiple exons (multi-exon skipping) within exons 45–55. Here, the *mdx*52 mouse is an indispensable animal model for the investigation of an exon-skipping strategy targeting this hot spot region.

Single-exon-skipping therapy

Based on the Leiden Muscular Dystrophy database (http://www.dmd.nl), exon skipping targeting exon 51 may be applicable to about 15% of patients with DMD having a deletion mutation. In the Netherlands, clinical trials of exon 51-skipping therapy for patients with the deletion of either exons 48–50, exons 49–50, exon 50, or exon 52 have been conducted.[39] In that study, 2OMeAOs were injected into the tibialis anterior (TA) muscle of the patients, and the efficacy of exon skipping, restoration of dystrophin expression, and improvement of MRI findings were reported, although the TA muscle function could not be evaluated because of local administration. Based on our on-going study of exon 51 skipping in the *mdx*52 mouse, a certain degree of improvement of muscle function is expected (Aoki *et al.*, unpublished data). In addition, the UK[40] and US/Japan are planning clinical trials of exon 51-skipping therapy using PMO.

In the Leiden Muscular Dystrophy database, relatively small-sized in-frame deletions, mainly including exons 50 and 51 (e.g. deletion of exons 45–51, 47–51, 48–51, 49–51, 50–51, 51, or 52) cause a high rate of DMD phenotypes (56–100%) rather than the BMD phenotype.[41] The mechanism underlying the high ratio of DMD phenotypes despite the in-frame mutation remains unclear, but the hinge 3 region coded by exons 50–51 of the *DMD* gene might have an important functional role in dystrophin. On the other hand, larger deletions including exons 50–51 (e.g. deletion of exons 45–53 or 45–55) more frequently present with a BMD phenotype.[41] Thus, hinge 3 might bestow flexibility on the protein structure, and when hinge 3 is absent, the longer spans between hinges might become fragile to mechanical stress. However, we also need to point out that gene deletion should be confirmed not only on a genomic DNA level but also an mRNA level.

Multi-exon-skipping therapy

As described above, exon 51-skipping therapy may be feasible for up to 15% of DMD patients having a deletion mutation, but this therapeutic method remains a "custom-made therapy," and large numbers of DMD patients will not benefit from it. We recently reported three unrelated patients with a deletion of exons 45–55, which covers the entire hot spot region, who have very mild skeletal muscle involvement and can still walk unassisted late in life.[42] Beroud *et al.* also described 15 patients having an exon 45–55 deletion who had very mild or asymptomatic skeletal muscle involvement.[43] Furthermore, when we examined the number of patients having deletions within exons 45–55 in the Leiden Muscular Dystrophy database combined with previous data,[42,43] the deletion of exons 45–55 produced a BMD phenotype in 97% of cases, which is second only to the percentage of BMD phenotypes due to deletion of exons 47–49.[43] If multi-exon skipping of exons 45–55 is feasible, not only approximate 60% of DMD but also severe BMD cases having a deletion within the hot spot may be treatable. We recently induced exons 45–55 skip-

ping by injection of mixtures of 10 PMOs in the anterior tibialis muscle of *mdx*52 mice and confirmed that multi-exon-skipping is feasible (Aoki *et al.*, unpublished data).

One of the difficulties of multi-exon skipping is the need to avoid the formation of duplex AOs. The affinity of PMOs for duplex formation is much stronger than that of DNA or RNA, and once a duplex PMO is formed, the efficacy of exon-skipping may be greatly decreased or an immune response might be induced. Another problem is that the efficacy of multi-exon skipping might be lower than that of single-exon skipping because many different splicing products could be produced. Thus, the design of each AO and their combinations are very important. However, there are advantages in exons 45–55-skipping therapy: we can treat up to 60% of DMD deletion patients using the same mixture of AOs if the mixture of AOs for multi-exon skipping is regarded as one pharmaceutical agent by the FDA and its Japanese counterpart PMDA. Even partial products for multi-exon skipping, which lack exons 45–46, 45–47, 45–48, 45–49, or 47–49, might give positive effects because each deletion causes the BMD phenotype rather than the DMD phenotype. Concerning the mutations outside of exons 45–55 in the *DMD* gene, at least in the Leiden database, 90% have deletion of exon(s) corresponding to the N- or C-terminal region of dystrophin,[13,41] 80% of DMD patients having a duplication as well.[41]

ISSUES OF EXON-SKIPPING THERAPY FOR DMD AND IMPACT ON OTHER DISORDERS

Issues remaining in exon-skipping therapy

One of the issues that accompanies exon-skipping therapy is whether the efficacy of skipping differs among organs or tissues. Systemic administration of 2OMeAO or PMO produced restoration of dystrophin expression that was much lower in the heart than in skeletal muscle.[20,35] Considering that many DMD patients die of cardiac complications such as heart failure or lethal arrhythmias, improvement of the efficacy of AOs in cardiac muscle is very important. It is unclear why the uptake of AOs in the cells of cardiac and skeletal muscle is different; however, it is intriguing to note that cardiac muscle cells have a single nucleus, unlike skeletal muscle cells. Therefore, damaged but living multi-nucleated muscle fibers may uptake PMO, but damaged cardiomyocytes may not survive and are soon replaced by fibrous tissues. To improve the efficacy of its introduction into cardiac muscle cells, injection of PMO combined with a microbubble contrast agent using diagnostic ultrasound has been proposed.[44] Another way to increase effectiveness is to use PPMO; once-a-day administration of PPMO to *mdx* mice for 4 days produced high restoration of dystrophin expression in cardiac muscle.[29] However, whether PPMO causes dose-dependent cytotoxicity or not should be examined.

We also need to consider another issue: each AO may or may not be considered a different pharmaceutical agent by the FDA or its counterparts. Further, even if the multi-exon-skipping from exon 45 to 55 is established, it is not applicable to all patients with DMD having a deletion, and a specific AO targeted to each type of mutation needs to be designed. Moreover, the costs for development of each AO and its clinical trials will be enormous if the FDA considers each AO to be a different drug. Therefore, it is expected that the FDA and its counterparts will consider PMOs as one drug, even if their sequences are different. Another big difficulty is that exon-skipping therapy by AOs modifies the splicing process of pre-mRNA for a limited period of time but does not affect the genome DNA itself; therefore, the efficacy of the treatment is finite and repeated administration will be needed.

Impact on other diseases

Duchenne muscular dystrophy is one of the plausible candidates for exon-skipping therapy because the phenotype of dystrophin-deficiency shows a heterogeneity from severe DMD phenotypes to asymptomatic cases and the correlation between genotype and phenotype has been well investigated on the basis of analysis of the molecular structure of dystrophin. The attempt of exon-skipping in DMD may provide a useful platform to develop experimental therapies for many other disorders, including manipulation of splicing of the muscle-specific chloride channel *ClC1* gene in myotonic dystrophy[45] and the *SMN2* gene of spinal muscular atrophy type 1,[46] switching of isoforms of the TNFα type 2 receptor gene, *TNFRSF1B*, in rheumatoid arthritis,[47] or knockdown of the collagen type 7 gene, *COL7A1* in epidermolysis bullosa.[47] Thus, the success of research on exon-skipping therapy and the clinical trials for DMD might have a large impact on the development of therapy for other disorders.

CONCLUSIONS

Exon-skipping therapy for DMD has rapidly advanced with newly developed AOs, especially PMO, and better animal models. Various issues accompanying this therapy, including the introduction, efficacy, and toxicity of AOs, remain prior to human clinical trials, but the ethical hurdles might be lower than those for gene therapy using viral vectors or stem cell transplantation therapy. This therapy could also be appropriate to patient populations with other disorders, and therefore is expected to be applicable to some hereditary neuromuscular disorders.

ACKNOWLEDGEMENTS

This study was supported by Health Sciences Research Grants for Research on Psychiatric and Neurological Diseases and Mental Health (H12-kokoro-025, H15-kokoro-021, H18-kokoro-019), the Human Genome and Gene Therapy (H13-genome-001, H16-genome-003), and Health and Labor Sciences Research Grants for Translation Research (H19-translational research-003) from the Ministry of Health, Labor and Welfare of Japan, and Grants-in-Aid for Scientific Research from the Ministry of Education, Science, Sports and Culture of Japan (to S.T.).

REFERENCES

1. Hoffman EP, Brown RHJ, Kunkel LM. Dystrophin: the protein products of the Duchenne muscular dystrophy locus. *Cell* 1987; **51**: 919–928.
2. Yoshimura M, Sakamoto M, Ikemoto M *et al.* AAV vector-mediated microdystrophin expression in a relatively small percentage of mdx myofibers improved the mdx phenotype. *Mol Ther* 2004; **10**: 821–828.
3. Ikemoto M, Fukuda S, Uezumi A *et al.* Autologous transplantation of SM/C-2.6(+) satellite cells transduced with micro-dystrophin CS1 cDNA by lentiviral vector into mdx mice. *Mol Ther* 2007; **15**: 2178–2185.
4. Dezawa M, Ishikawa H, Itokazu Y *et al.* Bone marrow stromal cells generate muscle cells and repair muscle degeneration. *Science* 2005; **309**: 314–317.
5. Welch EM, Barton ER, Zhuo J *et al.* PTC124 targets genetic disorders caused by nonsense mutations. *Nature* 2007; **447**: 87–91.
6. Yeung EW, Whitehead NP, Suchyna TM *et al.* Effects of stretch-activated channel blockers on [Ca2+]i and muscle damage in the *mdx* mouse. *J Physiol* 2005; **562**: 367–380.
7. Wilton SD, Dye DE, Blechynden LM, Laing NG. Revertant fibres: a possible genetic therapy for Duchenne muscular dystrophy?. *Neuromuscul Disord* 1997; **7**: 329–335.
8. Crawford GE, Lu QL, Partridge TA *et al.* Suppression of revertant fibers in mdx mice by expression of a functional dystrophin. *Hum Mol Genet* 2001; **10**: 2745–2750.
9. Lu QL, Morris GE, Wilton SD *et al.* Massive idiosyncratic exon skipping corrects the nonsense mutation in dystrophic mouse muscle and produces functional revertant fibers by clonal expansion. *J Cell Biol* 2000; **148**: 985–996.
10. Yokota T, Lu QL, Morgan JE *et al.* Expansion of revertant fibers in dystrophic mdx muscles reflects activity of muscle precursor cells and serves as an index of muscle regeneration. *J Cell Sci* 2006; **119**: 2679–2687.
11. Wilton SD, Fletcher S. Modification of pre-mRNA processing: application to dystrophin expression. *Curr Opin Mol Ther* 2006; **8**: 130–135.
12. Alter J, Lou F, Rabinowitz A *et al.* Systemic delivery of morpholino oligonucleotide restores dystrophin expression bodywide and improves dystrophic pathology. *Nat Med* 2006; **12**: 175–177.
13. Aartsma-Rus A, Janso N AA, Kaman WE *et al.* Antisense-induced multiexon skipping for Duchenne muscular dystrophy makes more sense. *Am J Hum Genet* 2004; **74**: 83–92.
14. Melis MA, Cau M, Muntoni F *et al.* Elevation of serum creatine kinase as the only manifestation of an intragenic deletion of the dystrophin gene in three unrelated families. *Eur J Paediatr Neurol* 1998; **2**: 255–261.
15. Schwartz M, Duno M, Palle AL *et al.* Deletion of exon 16 of the dystrophin gene is not associated with disease. *Hum Mutat* 2007; **28**: 205.
16. Wilson C, Keefe AD. Building oligonucleotide therapeutics using non-natural chemistries. *Curr Opin Chem Biol* 2006; **10**: 607–614.
17. Karkare S, Bhatnagar D Promising nucleic acid analogs and mimics: characteristic features and applications of PNA, LNA, and morpholino. *Appl Microbiol Biotechnol* 2006; **71**: 575–586.
18. Karkare S, Bhatnagar D Promising nucleic acid analogs and mimics: characteristic features and applications of PNA, LNA, and morpholino. *Appl Microbiol Biotechnol* 2006; **71**: 575–586.
19. Lu QL, Rabinowitz A, Chen YC *et al.* Systemic delivery of antisense oligoribonucleotide restores Dystrophin expression in body-wide skeletal muscles. *Proc Natl Acad Sci USA* 2005; **102**: 198–203.
20. Wells DJ. Therapeutic restoration of dystrophin expression in Duchenne muscular dystrophy. *J Muscle Res Cell Motil* 2006; **27**: 387–398.
21. Cartegni L, Chew SL, Krainer AR. Listening to silence and understanding: nonsense exonic mutations that affect splicing. *Nat Rev Genet* 2002; **3**: 285–298.
22. Lu QL, Mann CJ, Lou F *et al.* Functional amounts of dystrophin produced by skipping the mutated exon in the mdx dystrophic mouse. *Nat Med* 2003; **9**: 1009–1014.
23. Wee KB, Pramono ZA, Wang JL *et al.* Dynamics of co-transcriptional pre-mRNA folding influences the induction of dystrophin exon skipping by antisense oligonucleotides. *PloS ONE* 2008; **26**: e1884.
24. Artsma-Rus A, Janson AA, Kaman WE *et al.* Therapeutic antisense-induced exon skipping in cultured muscle cells from six different DMD patients. *Hum Mol Genet* 2003; **12**: 907–914.

25. Arechavala-Gomeza V, Graham LR, Popplewell LJ *et al.* Comparative analysis of antisense oligonucleotide sequences for targeted skipping of exon 51 during dystrophin pre-mRNA splicing in human muscle. *Hum Gene Ther* 2007; **18**: 798–810.
26. Grounds MD, Radley HG, Lynch GS *et al.* Towards developing standard operating procedures for pre-clinical testing in the mdx mouse model of Duchenne muscular dystrophy. *Neurobiol Dis* 2008; **31**: 1–19.
27. Wells KE, Flrcher S, Mann CJ *et al.* Enhanced in vivo delivery of antisense oligonucleotides to restore dystrophin expression in adult mdx mouse muscle. *FEBS Lett* 2003; **552**: 145–149.
28. Fletcher S, Honeyman K, Fall AM *et al.* Dystrophin expression in the mdx mouse after localized and systemic administration of a morpholino antisense oligonucleotide. *J Gene Med* 2006; **8**: 207–216.
29. Jearawiriyapaisarn N, Moulton HM, Buckley B *et al.* Sustained dystrophin expression induced by peptide-conjugated morpholino oligomers in the muscles of mdx mice. *Mol Ther* 2008; **16**: 1624–1629.
30. Goyenvalle A, Vulin A, Fougerousse F *et al.* Rescue of dystrophic muscle through U7 snRNA-mediated exon skipping. *Science* 2004; **306**: 1796–1799.
31. Shimatsu Y, Katagiri K, Furuta T *et al.* Canine X-linked muscular dystrophy in Japan ($CXMD_J$). *Exp Anim* 2003; **52**: 93–97.
32. Shimatsu Y, Yoshimura M, Yuasa K *et al.* Major clinical and histopathological characteristics of canine X-linked muscular dystrophy in Japan, $CXMD_J$. *Acta Myol* 2005; **24**: 145–154.
33. Yugeta N, Urasawa N, Fujii Y *et al.*. Cardiac involvement in Beagle-based canine X-linked muscular dystrophy in Japan ($CXMD_J$): electrocardiographic, echocardiographic, and morphologic studies. *BMC Cardiovascular Disord* 2006; **6**: 47.
34. Urasawa N, Wada MR, Machida N *et al.* Selective vacuolar degeneration in dystrophin-deficient canine Purkinje fibers despite preservation of dystrophin-associated proteins with overexpression of Dp71. *Circulation* 2008; **117**: 2437–2448.
35. Yokota T, Lu Q, Partridge T *et al.* Efficacy of systemic morpholino exon-skipping in Duchenne dystrophy dogs. *Ann Neurol* 2009; in press.
36. McClorey G, Moulton HM, Iversen PL *et al.* Antisense oligonucleotideinduced exon skipping restores dystrophin expression in vitro in a canine model of DMD. *Gene Ther* 2006; **13**: 1373–1381.
37. Araki E, Nakamura K, Nakao K *et al.* Targeted disruption of exon 52 in the mouse dystrophin gene induced muscle degeneration similar to that observed in Duchenne muscular dystrophy. *Biochem Biophys Res Commun* 1997; **238**: 492–497.
38. Kameya S, Araki E, Katsuki M *et al.* Dp260 disrupted mice revealed prolonged implicit time of the b-wave in ERG and loss of accumulation of beta-dystroglycan in the outer plexiform layer of the retina. *Hum Mol Genet* 1997; **6**: 2195–2203.
39. van Deutekom JC, Janson AA, Ginjaar IB *et al.* Local dystrophin restoration with antisense oligonucleotide PRO051. *N Engl J Med* 2007; **357**: 2677–2686.
40. Muntoni F, Bushby K, van Ommen G 128th ENMC International Workshop on "Preclinical optimization and Phase I/II clinical trials using antisense oligonucleotides in Duchenne muscular dystrophy" 22-24 October 2004, Naarden, The Netherlands. *Neuromuscul Disord* 2005; **15**: 450–457.
41. Yokota T, Pistilli E, Duddy W *et al.* Potential of oligonucleotide-mediated exon-skipping therapy for Duchenne muscular dystrophy. *Expert Opin Biol Ther* 2007; **7**: 831–842.
42. Nakamura A, Yoshida K, Fukushima K *et al.* Follow-up of three cases with a large in-frame deletion of exons 45-55 in the Duchenne muscular dystrophy (DMD) gene. *J Clin Neurosci* 2008; **15**: 757–763.
43. Beroud C, Tuffery-Giraud S, Matsuo M *et al.* Multi-exon skipping leading to an artificial DMD protein lacking amino acids from exons 45 through 55 could rescue up to 63% of patients with Duchenne muscular dystrophy. *Hum Mutat* 2007; **28**: 196–202.
44. Wang X, Liang HD, Dong B *et al.* Gene transfer with microbubble ultrasound and plasmid DNA into skeletal muscle of mice: comparison between commercially available microbubble contrast agents. *Radiology* 2005; **237**: 224–229.
45. Wheeler TM, Lueck JD, Swanson MS *et al.* Correction of ClC-1 splicing eliminates chloride channelopathy and myotonic in mouse models of myotonic dystrophy. *J Clin Invest* 2007; **117**: 3952–3957.
46. Wilton SD, Fletcher S. Splice manipulation therapies: opportunities and challenges. *Neuromuscl Disord* 2008; **18**: 831.
47. Aartsma-Rus A, van Ommen GJ. Antisense-mediated exon skipping: a versatile tool with therapeutic and research applications. *RNA* 2007; **13**: 1609–1624.

The FASEB Journal • Research Communication

Generation of transplantable, functional satellite-like cells from mouse embryonic stem cells

Hsi Chang,* Momoko Yoshimoto,*,† Katsutsugu Umeda,* Toru Iwasa,* Yuta Mizuno,* So-ichiro Fukada,‡ Hiroshi Yamamoto,‡ Norio Motohashi,§ Yuko-Miyagoe-Suzuki,§ Shin'ichi Takeda,§ Toshio Heike,*,[1] and Tatsutoshi Nakahata*

*Department of Pediatrics, Kyoto University Graduate School of Medicine, Kyoto, Japan; †Indiana University School of Medicine Wells Center for Pediatric Research, Indianapolis, Indiana, USA; ‡Department of Immunology, Graduate School of Pharmaceutical Science, Osaka University, Osaka, Japan; and §Department of Molecular Therapy, National Institution of Neuroscience, National Center of Neurology and Psychiatry, Tokyo, Japan

ABSTRACT **Satellite cells are myogenic stem cells responsible for the postnatal regeneration of skeletal muscle. Here we report the successful *in vitro* induction of Pax7-positive satellite-like cells from mouse embryonic stem (mES) cells. Embryoid bodies were generated from mES cells and cultured on Matrigel-coated dishes with Dulbecco's modified Eagle medium containing fetal bovine serum and horse serum. Pax7-positive satellite-like cells were enriched by fluorescence-activated cell sorting using a novel anti-satellite cell antibody, SM/C-2.6. SM/C-2.6-positive cells efficiently differentiate into skeletal muscle fibers both *in vitro* and *in vivo*. Furthermore, the cells demonstrate satellite cell characteristics such as extensive self-renewal capacity in subsequent muscle injury model, long-term engraftment up to 24 wk, and the ability to be secondarily transplanted with remarkably high engraftment efficiency compared to myoblast transplantation. This is the first report of transplantable, functional satellite-like cells derived from mES cells and will provide a foundation for new therapies for degenerative muscle disorders.—Chang, H., Yoshimoto, M., Umeda, K., Iwasa, T., Mizuno, Y., Fukada, S., Yamamoto, H., Motohashi, N., Yuko-Miyagoe-Suzuki, Takeda, S., Heike, T., Nakahata, T. Generation of transplantable, functional satellite-like cells from mouse embryonic stem cells. *FASEB J.* 23, 1907–1919 (2009)**

Key Words: long-term engraftment · secondary transplantation · high engraftment efficiency · self-renewal

DUCHENNE MUSCULAR DYSTROPHY (DMD; ref. 1) is a progressive, lethal muscular disorder (2) with no effective cure despite extensive research efforts. DMD results from mutations in the X-linked *dystrophin* gene (3). Dystrophin and its associated proteins function to link the intracellular actin cytoskeleton of muscle fibers to laminin in the extracellular matrix (4), thereby protecting myofibers from contraction-induced damage (5). Skeletal muscle fibers are continuously regenerated following exercise and injuries when satellite cells (6) are induced to differentiate into myoblasts that form myotubes and replace the damaged myofibers (7, 8). This muscular regeneration is observed at a much higher frequency in DMD patients (9). Continuous damage to myofibers and constant activation of resident satellite cells due to loss of dystrophin leads to the exhaustion of the satellite cells (10, 11), and the eventual depletion of satellite cells is primarily responsible for the onset of DMD symptoms.

Successful transplantation of normal satellite cells into the skeletal muscle of DMD patients may enable *in situ* production of normal muscle tissue and create a treatment option for this otherwise fatal disease. A recent report has shown that the transplantation of satellite cells collected from mouse muscle tissues can produce muscle fibers with normal dystrophin expression in mdx mice (12-14), a model mouse for DMD (15). This study suggests that stem cell transplantation may be a viable therapeutic approach for the treatment of DMD (16).

Satellite cells are monopotent stem cells that have the ability to self-renew and to differentiate into myoblasts and myotubes to maintain the integrity of skeletal muscle (17). Satellite cells lie dormant beneath the basal lamina and express transcription factors such as Pax3 (13, 18) and Pax7 (19). Pax7, a paired box transcription factor, is particularly important for satellite cell function. A recent study of *Pax7-null* mice revealed that Pax7 is essential for satellite cell formation (19) and that the *Pax7-null* mice exhibit a severe deficiency in muscle fibers at birth and premature mortality with complete depletion of the satellite cells. Surface markers such as M-cadherin and c-met (20) are also expressed by satellite cells. However, these markers are not specific to satellite cells because they are also expressed in the cerebellum (21) and by hepatocytes (22). To specifically identify quiescent satellite cells, a

[1] Correspondence: Department of Pediatrics, Kyoto University Graduate School of Medicine, 54 Syogoin Kawahara-cho Sakyo-ku, Kyoto 606-8507, Japan. E-mail: heike@kuhp.kyoto-u.ac.jp

doi: 10.1096/fj.08-123661